2D Nonlinearity Simulation of the Vertical Hall Sensor using SESES

Ch. Schott, Z. Randjelovic, J.-M. Waser and R. S. Popovic

Institute for Microsystems, EPFL-DMT, CH-1015 Lausanne, Switzerland
Phone: +41-21-693-6774, Fax: +41-21-693-6670, E-Mail: christian.schott@epfl.ch

Buried silicon vertical Hall devices have been accurately simulated in 2D under the condition of a varying magnetic field up to 2 Tesla using the numerical FEM device simulator SESES™. A field dependent Hall scattering factor allows for the first time to take effects of the magnetic field on the material properties into account. Comparing simulated values of input resistance and sensitivity for different geometry to measurements from real devices demonstrates the correct implementation of both, geometry-related and material non-linearity effects. This approach offers an efficient way for future design of highly linear devices.

Keywords : Hall device, Vertical Hall sensor, Simulation, SESES, Non-linearity simulation.

INTRODUCTION

Buried Hall devices made of semiconductor material feature a more or less nonlinear behavior when measuring fields higher than some gauss. Non-linearity is generally defined by the change of a device's sensitivity with the magnetic field and is caused by three different effects:

a) the Junction-Field effect modulates the thickness of the depletion layer surrounding a buried device. This effect is reduced, by applying a polarization technique described in [1]. It can be neglected for further considerations.
b) a geometrical effect depending on the geometry of the device and causing an increase of sensitivity with the magnetic field.
c) a material effect depending on the scattering mechanisms in the semiconductor causing a decrease of sensitivity with the magnetic field.

Our goal is to match material and geometrical parameters in the vertical Hall sensor (VHS) with an appropriate design. In such a way we can take advantage from mutual cancellation and obtain a highly linear behavior. Since the description of a real vertical Hall device by analytic equations is difficult, we chose a numerical approach with the FEM device simulator SESES.

SIMPLIFICATION OF THE MODEL

In order to limit the number of parameters, we use a model where the full set of basic equations for semiconductor device operation are reduced by the following assumptions:

a) room temperature
b) no dielectric displacement currents
c) no inductive currents
d) no space charge
e) no generation and recombination of carriers
f) no gradients in carrier densities
g) magnetic field perpendicular to current density

The only equation left is the current density equation representing the base for the simulations of our devices.

$$\vec{J} = \sigma\vec{E} + \sigma\mu_H\left[\vec{E}\times\vec{B}\right] \tag{1}$$

PHYSICS OF NONLINEARITY

First of all we give a brief introduction to the mechanisms leading to non-linearity. We consider the charge carriers as being non-degenerate and the magnetic induction up to 2 Tesla as low [2]. We also assume acoustic phonon scattering as the prevailing mechanism.
Taking a closer look at the physical parameters, we can see how they are modified in the presence of a magnetic field and how they are related to input resistance and Hall voltage in our model.

- The material's conductivity σ in direction of the local electric field decreases quadratic with the magnetic field.

$$\sigma(B) = \sigma_0\left(1 - r_3\mu^2B^2\right) \tag{2}$$

This is called the geometrical magnetoresistance effect (corbino magneto-resistive effect) and is due to the deflection of the current lines by the Lorentz force. This parameter does not have to be taken into account, since it is developed intrinsically by the finite element approximation. In a corbino disc where no Hall electric field is present this effect increases the input resistance about 15% at 2 Tesla, whereas in an ideally long device it does not appear since the current is not deflected. For real devices it will be somewhere in between these values.

- The material's resistivity ρ in the direction of the local current density increases quadratic with the magnetic field.

$$\rho(B) = \rho_0\left(1 + \left(r_3 - r_2^2\right)\mu^2B^2\right) \tag{3}$$

This is called the material magnetoresistance effect and is due to a statistical distribution of the velocity of the charge carriers travelling through the material [2]. It does not depend on the device geometry and is present in any semiconductor material. This effect has to be explicitly implemented in the model. It leads to an increase of the input resistance of about 3.3% at 2 Tesla.

Both of these parameters depend upon the square of the mobility and the magnetic inductance. Their variation can be directly observed by an increase of the device's resistance between the biasing contacts.

- The Hall mobility μ_H

$$\mu_H(B) = \mu_{H0}\left(1 - \left(\frac{r_4}{r_2} - r_3\right)\mu^2 B^2\right) \qquad (4)$$

$$\mu_{H0} = r_2\mu$$

The Hall mobility describes how easy charge carriers can travel in a direction transverse to the current density under the influence of the Lorentz force in a magnetic field. The parameter also has to be explicitly implemented in the model.

- The Hall coefficient R_H is the physical parameter describing the efficiency of creating a Hall electric field in the material.

$$R_H(B) = \mu_H(B)\rho(B) \qquad (5)$$

Its dependence on the magnetic induction is already taken charge of by the implementation of Hall mobility and and resistivity.

- The geometrical correction factor is a parameter taking the geometry (length, width of active area and contacts) into account.

$$G(B) = G_0 + \frac{1 - G_0}{3}\mu^2 B^2 \qquad (6)$$

It describes the Hall voltage of a non-ideally long device in comparison with an ideally long device. It can be interpreted as the parameter taking the short-circuiting effects of current and Hall electrodes into account. It does not have to be implemented, since it is intrinsic to the finite element solution.

These three parameters have a direct influence on the output signal of a device, which is the Hall voltage. All of them do also depend on the square of the magnetic induction.

- The last parameter we use in the given formulae is the electron mobility in low doped silicon at room temperature having a value of approximately $\mu = 0.15$ m^2/Vs. It is invariant under the conditions mentioned above.

THE PHYSICAL MODEL IN SESES

For modeling a vertical Hall sensor we are using the program SESES (**SE**miconductor **S**Ensor and actuator Simulation) which works with a finite element algorithm. We applied the kernel r2d for solving a problem for current continuity in continua. The basic equation for such a problem is the current continuity equation

$$\bar{\nabla}\bar{J} = 0 \qquad (7)$$

The current density J is related to the electric potential by the infinitesimal version of Ohm's law

$$\bar{J} = -\sigma\bar{\nabla}\Psi \qquad (8)$$

When a magnetic induction is applied to a device, Ohms Law is extended by a Lorentz term

$$\bar{J} = -\sigma\left(\bar{\nabla}\Psi + \mu_H\bar{\nabla}\Psi \times \bar{B}\right) \qquad (9)$$

SESES offers the physical model "Hall" to solve such a problem. In this model conductivity is not only related to mobility μ, temperature T and doping concentration D, but also to the magnetic field

$$\sigma(D,T,B) = \frac{q\mu(D,T)D}{1 + \left(\left|\bar{B}\right|\mu_H(D,T)\right)^2} \qquad (10)$$

This formula is <u>not</u> the implementation of the geometrical magnetoresistance effect, but another representation of the material magnetoresistance effect as we desribed it in (3).

The Hall mobility is defined by the mobility with an adjustable scattering factor μ_{scat}

$$\mu_H(D,T) = \mu_{scat}\mu(D,T) \qquad (11)$$

Contrary to the requirements of equation (4) is μ_H here not explicitly implemented in relation to the magnetic induction. This step is explained in the next section.

IMPLEMENTATION OF NON-CONSTANT HALL MOBILITY

As we can see from semiconductor physics, does a constant scattering factor not satisfy an accurate simulation. Theoretically the Hall scattering factor has a value of r_2=1.18 at a field of 0 Tesla and reaches a constant value of about 0.88 at very high fields [2]. Since the Hall factor R_H is directly related to the Hall mobility, we can expect an error of about 30% if not varying it with the value of the magnetic induction.

For a magnetic induction of up to 2T R_H can be approximated in a quadratic dependence on the mobility and the magnetic induction (eq. 3,4,5). This variation was

for the first time taken into account in our model by calculating at each field value a different Hall scattering factor. In accordance with its quadratic dependence on the magnetic induction (eq. 4), we defined it as

$$\mu_{scat}(B) = a(1 - bB^2) \qquad (12)$$

In this equation a and b are constants calculated by the scattering parameters.

THE DEVICE AND ITS MODEL

Figure 1 shows a Vertical Hall Sensor (VHS) as it is realized in a technology with the active area open to the substrate. It is a device, which has been transformed from a brick-shape plate by a conformal mapping technique, so that after the transformation all electrical contacts can be placed at one side and it can be manufactured using microelectronic fabrication methods.

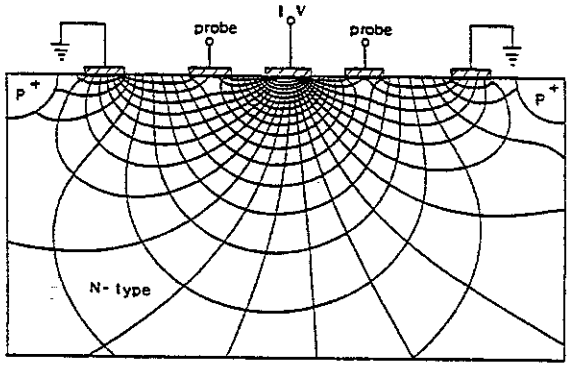

Figure 1 : The vertical Hall device has all electrical contacts on one side and shows a similar behavior to conventional Hall plates.

Such devices can be fabricated with different length of the current and/or Hall contacts giving them different characteristics in the magnetic field in analogy to conventional Hall plates. The issue of this paper is to demonstrate a possibility of simulating such devices with field dependent Hall mobility. For simplifying meshing and limiting computation time we restrained our simulation to two-dimensional models.

Figure 2 shows an example for the calculated potential in 2D presentation. In this simulation a constant current density was set over the surface of the current electrodes as boundary condition. The electrodes themselves are considered to be ideal conductors.

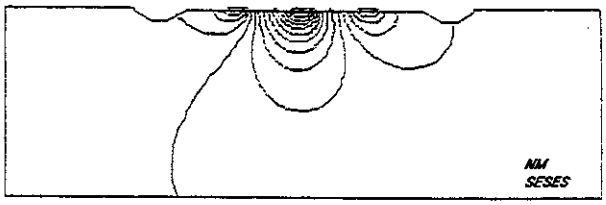

Figure 2 : Vertical Hall device showing the calculated potential lines at a field of 2 T. The two carved out trenches were used to model the ring gate giving the device its vertical geometry.

The zoom in view of figure 3 shows the regions with automatic mesh refinement around the center electrode providing convergence of the solution in areas of large current densities and large voltage gradients.

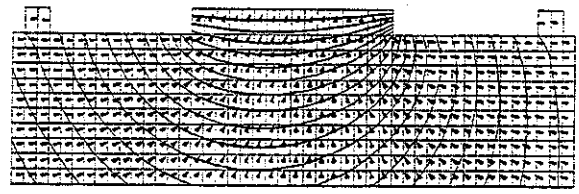

Figure 3 : Zoom of the center of the VHS as it was used in the simulations. At the surface to the left and the right the short Hall contacts can be seen. Smooth lines of equal current density and cones indicating the current direction show the accurate implementation of the device geometry.

Special attention was paid to the implementation of the contact surfaces with respect to the active device region. For stability reasons is the surface of the real device covered by a shallow p-layer. Between the electrical contacts this layer extends a region into the active material which is depleted from charge-carriers. Since its thickness is not exactly know, we simulated three variations with the contacts above the surface, embedded in it and even with it. In figures 4 and 5 we can see the simulated results for these three possibilities in comparison with measurements of a corresponding real device. The absolute values of input voltage and sensitivity show clearly that the "above" implementation is the correct one, which means, that the depletion layer reaches deeper into the substrate than the highly doped contact.

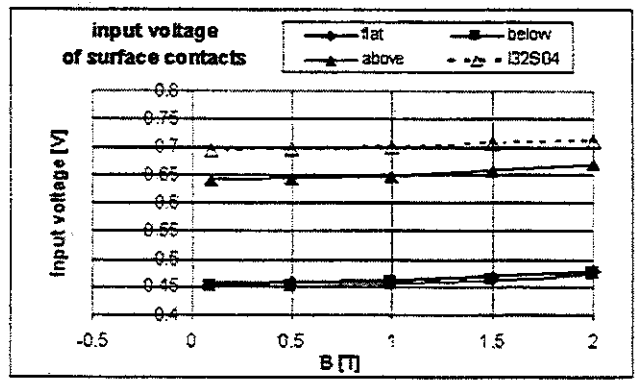

Figure 4 : Input voltage simulation for electrode embedding flat, above and below the surface. In the "above" model the simulated result correspond quite accurately to the ones obtained from a real device. The difference between "above" and the other two can be interpreted as the presence of a serial resistance between the contacts and the bulk material.

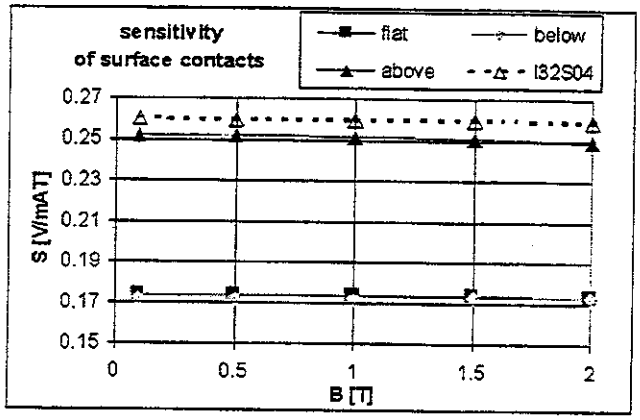

Figure 5 : Sensitivity results of the simulation for electrode embedding flat, above and below the surface. The "above" model here also corresponds to the best to the measurements on a real device.

The geometry of the devices used for the simulations is shown in figure 6. One was designed with very short contacts so that the influence of geometry-related non-linearity is restricted to a minimum, whereas another one was designed with much longer contacts for mutual compensation between both types of non-linearity. The other two devices were made with mixed contact length, long current contacts, short Hall contacts and vice versa.

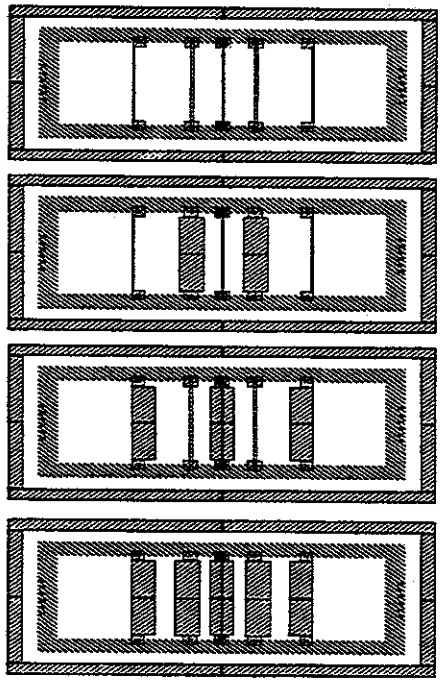

Figure 6 : Layout of the four devices which have been implemented in SESES and then compared to real devices. The top one with 4 microns long contacts features only material non-linearity, whereas the bottom one with 32 micron long contacts takes advantage of mutual elimination between material and geometry-related non-linearity. The two devices in between have 4 micron long current contact and 32 micron long Hall contacts and vice versa. They are supposed to feature similar non-linearity, but different input resistance behavior.

In the following we will discuss the results of the simulated devices to measurements of the manufactured ones. A Hall sensor as a quadrupole element features basically two voltages of interest, which are the input voltage and the Hall voltage. In our analysis we examine their absolute values and their variation under the presence of a magnetic field

RESULTS

The above mentioned four devices have been modeled in SESES and the simulation results are shown in this section always comparing them to measurement results of the real devices. In a first step we compare the level of input voltage and sensitivity to show that the initial parameters without the influence of a magnetic field as well as the geometry have been correctly implemented. In a second step we show the results obtained with constant Hall mobility and in a third the ones with field dependent Hall mobility. Finally we will show and interpret the results for the mixed contact devices.

a) Input voltage :

Figure 7 shows the potential difference appearing between the two current electrodes, when a constant current is applied. For the sensor with very short contacts and the one with very long contacts the simulated values correspond well to the measured ones. This proves a correct implementation of the meshed geometry and the correct value for the conductivity.

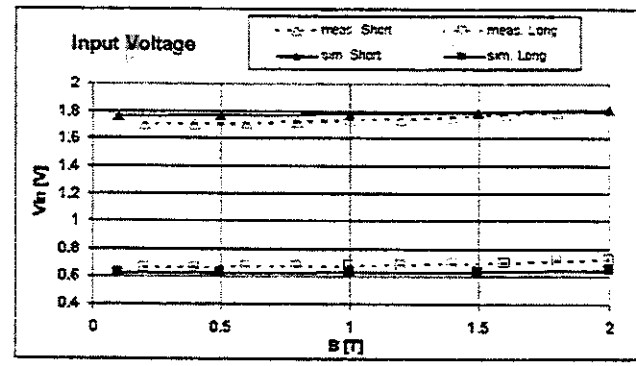

Figure 7: measured and simulated input voltage for the Hall devices with very short and very long contacts show the correct implementation of the model.

b) Sensitivity :

The absolute sensitivity in figure 8 for the same two devices shows that we set the correct term for the Hall mobility, and that the geometry of the devices was correctly simulated. If we consider the device with the small contacts as being close to an ideally long device, we obtain for the

one with the long contacts a geometrical correction factor of 0.7, since its sensitivity is about 30% smaller.

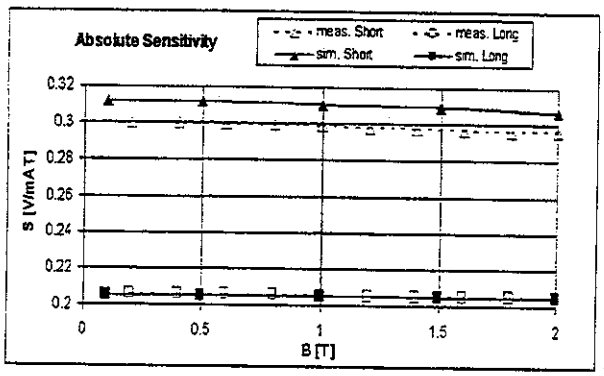

Figure 8 : measured and simulated sensitivity

c) The change of sensitivity in the magnetic field with constant scattering factor

In the next step the behavior of sensitivity in the magnetic field is examined. The first simulation has been carried out setting the Hall mobility to a constant value independent of the magnetic induction.

$$\mu_{scatt}(B) = 1.1 = const \qquad (13)$$

Using the value of 0.7 for the geometrical correction factor for the device with the long contacts, we calculate with equation (6) a positive geometric non-linearity of 1.3% at a field of 2 Tesla. Figure 9 compares the normalized results from simulation to the ones measured. By the difference in sensitivity between both devices at 2 Tesla, we can see that they correspond roughly to the theoretical prediction.

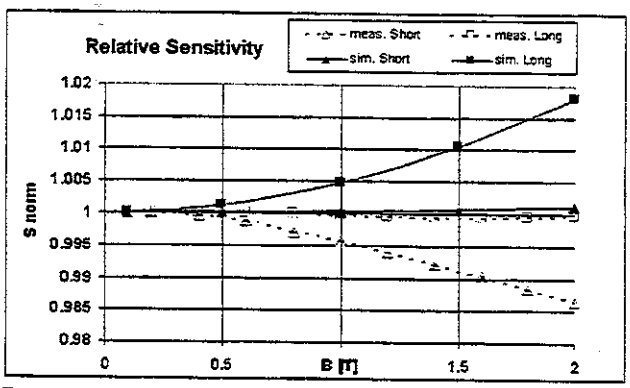

Figure 9 : The relative change of sensitivity in the magnetic field does not exactly correspond to the measured one when the Hall scattering factor is kept constant. The geometrical influence creates the same difference between the two simulated and the two measured values.

On the other hand are the simulated values too high. This problem is solved in the next chapter, introducing the field dependent scattering factor.

d) The change of sensitivity in the magnetic field with field-dependent scattering factor

As we explained before, does the Hall scattering factor determine the movement of charge carriers under the influence of the Lorentz force. It appears in formula (5) as part of the Hall voltage generating term. We do now apply a scattering factor varying with the magnetic induction

$$\mu_{scatt}(B) = 1.1\left(1 - 0.0047B^2\right) \qquad (14)$$

The results of the simulation after this modification can be seen in figure 10. The sensitivity of both devices does now correspond to the measured values.

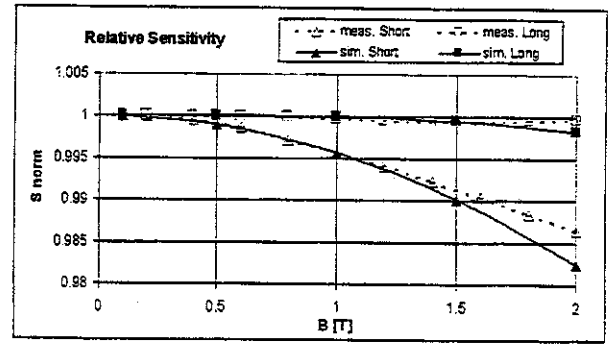

Figure 10 : After incorporating the field dependent quadratic variation of the Hall scattering factor, the simulated results correspond well to the measurements.

This step demonstrates the correctness of the theoretical assumptions, since the simulation results only match the real behavior of the devices when all physical characteristics are taken into account.

e) The change of input voltage in the magnetic field

The behavior of the variation of the input voltage of the devices in the magnetic field is shown in figure 11. Here the simulated and the measured results do not match.

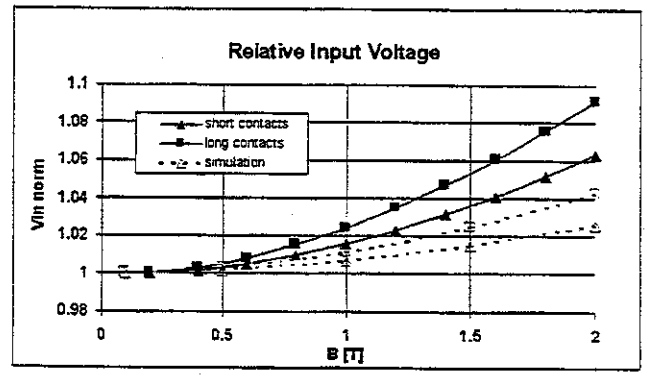

Figure 11 : relative input voltage

This is probably due to an unmatched factor in eq. 10. We have seen that the physical magnetoresistance effect alone increases the input resistance at 2 Tesla already 3.3% which can be considered as value for the short contact device. The

graph shows, that for the simulation the factor in eq. 10 has to be multiplied by a factor 3.

f) Devices with mixed contact length

The two devices shown in the middle of figure 7 have each one pair of short and one pair of long contacts.
Since the input resistance is more strongly related to the length of the input contacts than to the length of the Hall contacts, do the two devices show simulated and measured values which correspond roughly to the values of the first two devices (fig. 12)

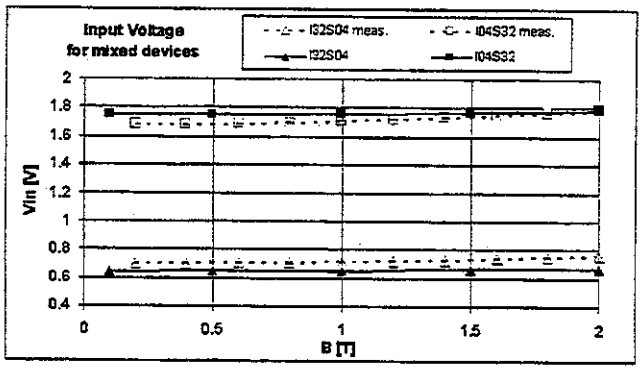

Figure 12 : Measured and simulated input voltage of the devices with mixed contact length depend mainly upon the length of the current electrodes and are almost independent from the length of the Hall electrodes.

Theoretically both devices should have the identical sensitivity as long as the geometry of the active region and the ratio of contact length to device circumference is identical. Their value of sensitivity is supposed to lie exactly in between the devices with two short and two long contacts. Figure 13 shows that this is for the measurements as for the simulations the case.

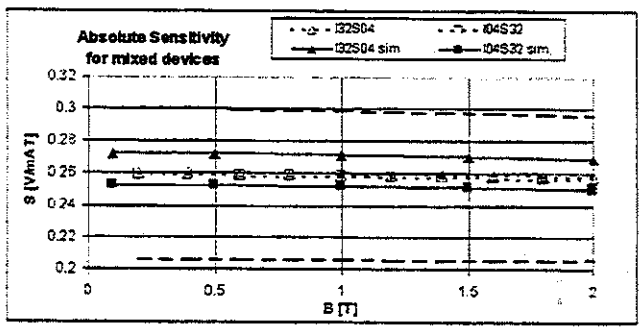

Figure 13 : The sensitivity of the two mixed devices is about the same, since it depends upon the geometrical correction factor which does not make a difference between current contacts and Hall contacts. The two devices with two short and two long contacts are plotted as interrupted lines.

In figure 14, plotting the relative change of sensitivity with the magnetic field, it can be seen, that the geometrical correction factor is for both devices the same and lies in the middle between the two devices with extreme geometry.

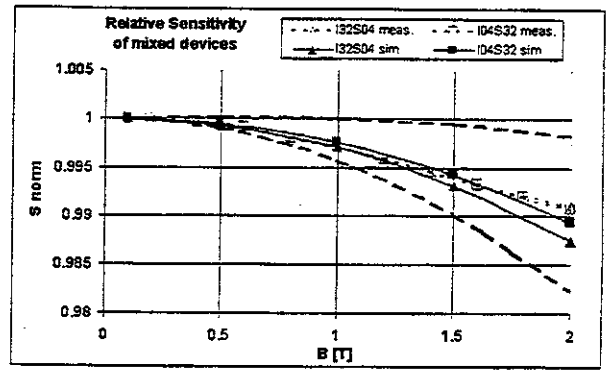

Figure 14 : The decrease of sensitivity for the two devices with mixed contact length is very similar and lies between the two extreme devices. This is also due to the similar geometrical correction factor.

CONCLUSION

The accurate implementation of vertical Hall devices with different geometry in the semiconductor device simulator SESES was demonstrated. A good correspondence between measured and simulated values for absolute and relative voltage and sensitivity for various contact lengths was shown. This was made possible by the implementation of a varying Hall scattering factor in the simulation model. The device with small current and sense contacts shows a high drop in sensitivity between 0 and 2 T due to prevailing material non-linearity. The device with the large contacts features an almost perfect annihilation between geometry and material effects. The implementation of two other devices with opposite contact length showing equal Hall voltages in the simulated results is another proof for the good performance of the model. However, a mismatch between measurement and calculation for the relative change of the input voltage reveals that the material magnetoresistance effect is not yet correctly implemented in the simulation program. Our future work will be directed towards the completion of the physical model in collaboration with our research project partners from Numerical Modelling.

REFERENCES

[1] Ch. Schott and R. S. Popovic, *Linearizing Integrated Hall Devices*, Transducers 97, Chicago, USA, June 16-19, 1997

[2] R.S. Popovic, *Hall Effect Devices*, Adam Hilger, Bristol, Philadelphia and New York, 1991.

[3] Z. Randjelovic, Ch. Schott and R. S. Popovic, *Modelling and Simulation of a High Accuracy Magnetometer*, Microsim 97, Lausanne, Switzerland

[4] SESES user manual, Chapter 1 and 6